Serotonin 5-HT 1A Receptor Biased Agonists Induce Different Cerebral Metabolic Responses: A [18 F]-Fluorodesoxyglucose Positron Emission Tomography Study in Conscious and Anesthetized Rats

Élise Levigoureux, Benjamin Vidal, Sylvain Fieux, Caroline Bouillot, Stéphane Emery, Adrian Newman-Tancredi, Luc Zimmer

Serotonin 5-HT$_{1A}$ Receptor Biased Agonists Induce Different Cerebral Metabolic Responses: A [^{18}F]-Fluorodesoxyglucose Positron Emission Tomography Study in Conscious and Anesthetized Rats

Elise Levigoureux,[†,‡,#] Benjamin Vidal,[†,#] Sylvain Fieux,[†] Caroline Bouillot,[§] Stéphane Emery,[†,‡] Adrian Newman-Tancredi,[∥] and Luc Zimmer*[,†,‡,§]

[†]Université de Lyon, Université Claude Bernard Lyon 1, Lyon Neuroscience Research Center, CNRS UMR5292, INSERM U1028, Lyon 69677, France

[‡]Hospices Civils de Lyon, Lyon 69677, France

[§]CERMEP-Imaging Platform, Bron 69677, France

[∥]Neurolixis Inc, Dana Point, California 92629, United States

ABSTRACT: Serotonin 5-HT$_{1A}$ receptors constitute an attractive therapeutic target for various psychiatric or neurodegenerative disorders. These receptors are expressed in multiple brain regions on different neuronal populations and can be coupled with distinct G-protein subtypes; such functional diversity complicates the use of 5-HT$_{1A}$ ligands in several pathologies where it would be desirable to stimulate the receptors in a precise region. Therefore, using "biased agonists" able to target specifically certain subpopulations of 5-HT$_{1A}$ receptors would enable achievement of better therapeutic benefit. Several 5-HT$_{1A}$ receptor biased agonists are currently in development, including NLX-101 (aka F15599) and NLX-112 (aka F13640, befiradol), with preclinical data suggesting that they preferentially target different populations of 5-HT$_{1A}$ receptors. However, most previous studies used invasive and regionally limited approaches. In this context, [^{18}F]-fluorodesoxyglucose (FDG)-positron emission tomography (PET) imaging constitutes an interesting technique as it enables noninvasive mapping of the regional brain activity changes following a pharmacological challenge in conscious animals. We report here the evaluation of cerebral glucose metabolism following intraperitoneal injection of different doses of NLX-112 or NLX-101 in conscious or isoflurane-anesthetized rats. The biased agonists produced different metabolic "fingerprints" with distinct regional preferences, consistent with previous studies. At equal doses, the effect of NLX-101 was less marked than NLX-112 in the piriform cortex, in the striatum (in terms of inhibition), and in the pontine nuclei and the cerebellum (in terms of activation); furthermore, only NLX-112 increased the glucose metabolism in the parietal cortex, whereas only NLX-101 induced a clear activation in the colliculi and the frontal cortex, which may be related to its distinctive procognitive profile. Both agonist effects were almost completely unapparent in anesthetized animals, underlining the importance of studying serotonergic neurotransmission in the conscious state. In this regard, [^{18}F]FDG-PET imaging seems very complementary with other functional imaging techniques such as pharmacological MRI.

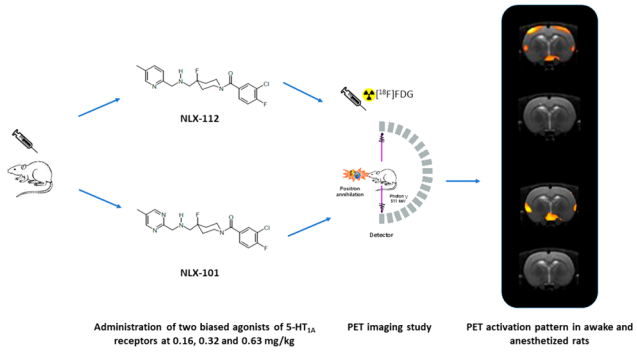

KEYWORDS: *serotonin, 5-HT$_{1A}$ receptors, biased agonism, functional selectivity, positron emission tomography, [^{18}F]FDG*

INTRODUCTION

The monoamine neurotransmitter serotonin (5-hydroxytryptamine [5-HT]), is derived from tryptophan and synthesized in both the central nervous system (CNS) and the periphery. At least 14 structurally and functionally distinct receptor subtypes have been identified, each of which mediates the neurotransmitter's effects through multiple downstream signaling molecules and effectors. Among them, the 5-HT$_{1A}$ receptor is involved in a wide range of physiological processes like cognition, behavior, movement, and pain modulation[1] and occupies a prominent place as a target for treatment of various psychiatric pathologies including mood disorders[2] and schizophrenia[3,4] and of neurodegenerative diseases, for example, Parkinson's disease[5] or Alzheimer's disease.[6] In the central nervous system, 5-HT$_{1A}$ receptors are expressed both as autoreceptors on cell bodies in the raphe nuclei, where they exert inhibitory influence on serotonergic tone,[7] and as postsynaptic heteroreceptors in cortical areas, hippocampus,

lateral septum, and hypothalamus.[8] In addition to this regional diversity, 5-HT_{1A} receptors can induce a wide range of intracellular responses.[9] As G-protein-coupled receptors (GPCRs) that interact with inhibitory G-proteins ($G_{i/o}$), they elicit adenylyl cyclase inhibition, resulting in decreased cyclic adenosine monophosphate (cAMP) production and protein kinase A (PKA) activity. Stimulation of 5-HT_{1A} receptors also activates G-protein-coupled inwardly rectifying potassium (GIRK) channels, which produce a fast hyperpolarization, and growth factor extracellular-signal-regulated kinase (ERK) pathways.[10]

Transduction pathways mediated by 5-HT_{1A} receptors can differ between brain regions[10] as a result of coupling to different G-protein subtypes.[11] This regional diversity is a key element in the recent pharmacological paradigm of "biased agonism", also known as "functional selectivity" or "agonist-directed signaling". Whereas agonists have been classically considered to activate all responses available to the receptor, the concept of biased agonism states that some agonists can stimulate distinct signaling responses among the different pathways interacting with the same receptor.[12] In the context of serotonin pharmacotherapy, this means that 5-HT_{1A} receptor biased agonists could preferentially activate certain receptors depending on their coupling state in specific brain regions, thus potentially optimizing therapeutic activity and reducing the occurrence of side effects.[10]

In this context, we focus here on two selective and high efficacy biased agonists of 5-HT_{1A} receptors: NLX-112 (also known as F13640 or befiradol) and NLX-101 (also called F15599). Previous *in vitro* studies showed that they preferentially stimulate different signaling pathways.[13,14] *In vivo* or *ex vivo* studies in animal also suggest that NLX-112 stimulates both presynaptic and postsynaptic receptors.[15,16] In contrast, NLX-101 is able to specifically target postsynaptic 5-HT_{1A} receptors at low dose, in particular in cortical brain regions.[13,17] However, the studies that most compellingly demonstrated the regional selectivity of NLX-112 and NLX-101 *in vivo* used invasive and regionally limited techniques, such as electrophysiology, microdialysis, or immunohistochemistry. In this context, our team recently compared these two biased ligands using pharmacoMRI (phMRI) in the rat[18] and in the cat[19] to map the central effects of NLX-112 and NLX-101 on BOLD signal in the whole brain *in vivo* and further supporting the postsynaptic cortical preference of NLX-101. These studies clearly demonstrated that two 5-HT_{1A} biased agonists can induce very different brain activation patterns, despite being close analogs in terms of chemical structure.[20] Nevertheless, these studies were performed in anesthetized animals, limiting the interpretation of results. Indeed, anesthetic agents, and notably isoflurane, are known to influence serotonergic neurotransmission and G-protein coupling.[21−23] Moreover, the blood-oxygen level dependent (BOLD) signal measured by fMRI is only indirectly related to neuronal activity,[24] and using other imaging techniques would bring additional information to fully understand the properties of biased ligands *in vivo*.

In this regard, positron emission tomography (PET) imaging with [^{18}F]FDG (fluorodesoxyglucose) is a suitable technique since it can be used to obtain brain activation patterns of CNS drugs without the need to anesthetize the animals. PET is a nuclear medicine imaging modality allowing the study of brain neurochemistry with unequaled sensitivity in a noninvasive way, thereby providing another translational method complementary to phMRI to evaluate the functional selectivity of different agonists. The PET radiotracer [^{18}F]FDG is able to quantify changes in brain activity that are reflected by changes of cerebral metabolic rate of glucose.[25]

The purpose of this study was twofold: (i) to define the brain activation profiles of the 5-HT_{1A} receptor biased agonists NLX-112 and NLX-101, based on glucose metabolism changes induced by the ligands at pharmacological doses (0.16, 0.32, and 0.63 mg/kg) in rat using [^{18}F]FDG PET imaging and (ii) to evaluate the influence of isoflurane anesthesia on 5-HT_{1A} receptors by comparing the brain activation pattern obtained in awake versus isoflurane-anesthetized animals. Our main hypotheses were that [^{18}F]FDG PET imaging would confirm previous preclinical data regarding the differences in regional selectivity between the ligands and add new information on their mechanism of action in awake animals (as opposed to previous phMRI studies that were performed in anesthetized animals). We also hypothesized that brain activation maps in awake and anesthetized animals would differ due to the strong disruption of neurotransmission during anesthesia, highlighting the usefulness of studying biased agonism *in vivo* in awake animals.

RESULTS AND DISCUSSION

Study Context and Methodology. The aim of this study was to map the changes of cerebral glucose metabolism induced by two selective 5-HT_{1A} agonists, NLX-112 and NLX-101, which though acting on the same receptor type with similar affinities and efficacies[20] differently activate intracellular signaling pathways.[13,14] As previous studies suggested that they preferentially target distinct subpopulations of 5-HT_{1A} receptors expressed in different brain regions,[14−17] our main hypothesis was that NLX-101 and NLX-112 would differently modify the regional [^{18}F]FDG uptake in the rat brain, underlining distinct effects on neuronal activity. [^{18}F]FDG PET imaging is a technique that can be used to measure neuronal activity changes induced by a serotonergic challenge in a noninvasive way, contrary to the aforementioned studies.[26−28] Furthermore, it can be performed on conscious animals, which makes it complementary to other imaging techniques such as functional MRI.[29] As previous preclinical studies investigated the regional selectivity of NLX-112 or NLX-101 in anesthetized animals, we performed PET-[^{18}F]FDG experiments both on conscious and anesthetized rats in order to further understand the impact of anesthesia when studying serotonergic neurotransmission and biased agonism. The agonists were injected at 3 pharmacologically relevant doses to evaluate the influence of dose on glucose utilization and possible regional preferences of the drugs. The doses of 0.16 mg/kg to 0.63 mg/kg and the route of administration were chosen based on previous preclinical studies.[30−35] Each rat was its own control and received each of the three doses of agonist and the saline solution in a randomized order. The interval between two acquisitions was at least 2 days, to ensure complete elimination of the molecules (the plasma half-life of NLX-112 in rat is about 1−2 h[31]). The amount of [^{18}F]FDG injected was calibrated to the weight of the animals, and these were fasted before the scans. The standardized uptake values in each scan were normalized to the mean radioactivity in the whole brain. This method was used in order to minimize the interscan variability, as it does not consider the possible changes in the peripheral glucose metabolism, a confounding factor when interpreting the

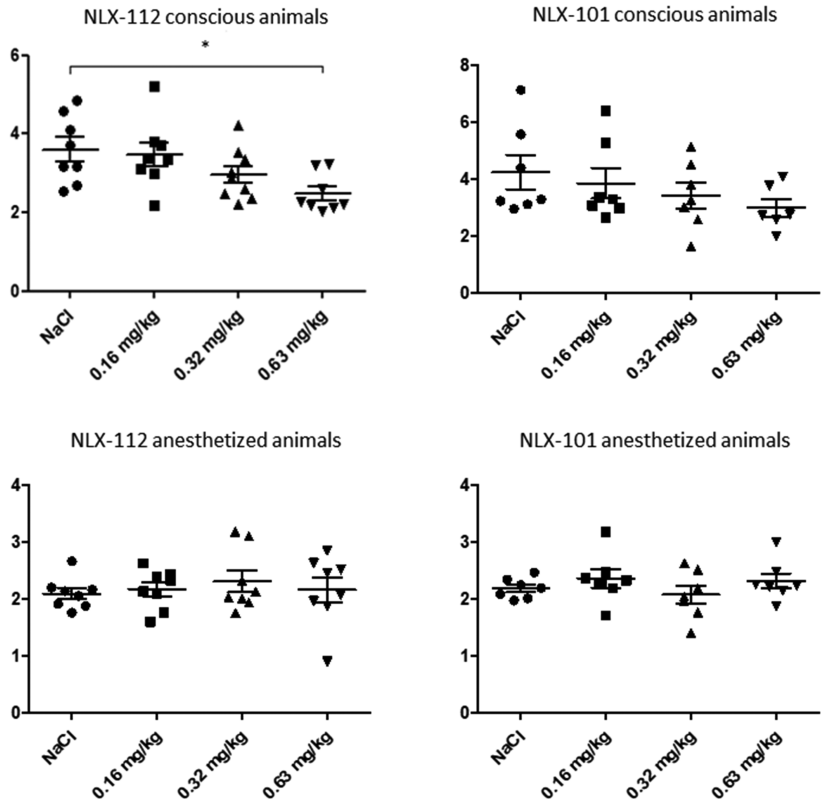

Figure 1. Mean whole-brain SUVs in conscious and anesthetized rats injected with NaCl, NLX-112, and NLX-101 at different doses (expressed as SUV, mean ± SD; *$p < 0.05$; one-way ANOVA with Bonferroni post hoc tests were performed using GraphPad Prism 5.0 software). Both NLX-112 and NLX-101 tended to decrease the whole brain uptake of [^{18}F]FDG proportionally to the dose in conscious animals.

cerebral glucose uptake in terms of changes in neuronal activity. Although this approach is the best way to compare the regional effects of central drugs on glucose uptake, it may also underestimate the global changes of brain metabolism. Therefore, we also measured the mean whole-brain standard uptake values (SUVs) for each condition (Figure 1). Both NLX-112 and NLX-101 tended to decrease the whole brain uptake of [^{18}F]FDG proportionally to the dose in conscious animals, suggesting that we underestimate their inhibitory effects on the global brain activity or that the drugs induce peripheral effects that can change the repartition of glucose uptake across the different organs. In this regard, it is known that 5-HT$_{1A}$ agonists can induce hyperglycemia.[36] As observed in conscious animals only, it could also be due to the behavioral effects of the drugs that tended to increase the motor activity and therefore the glucose consumption in the muscles.

PET Scans Performed in Conscious Rats. Before presenting in detail the specific effects of each agonist, general remarks can be made. First, both agonists produced local increases and decreases in [^{18}F]FDG uptake ratio in different regions. Such mixed effects are not surprising considering the diversity of neurons expressing 5-HT$_{1A}$ receptors, namely glutamatergic, GABAergic, or cholinergic neurons for post-synaptic receptors and serotonergic neurons for presynaptic receptors,[10] and the fact that 5-HT$_{1A}$ receptors can be coupled with various intracellular pathways across the brain.[11] Other studies also reported both decreases and increases of cerebral glucose metabolism following the administration of buspirone and 8-OH-DPAT.[37,38] A second general remark is that the changes were generally proportional to the doses administered. This is also consistent with a previous autoradiographic study with buspirone.[38]

The representative images of the voxel-based analysis of the effects of NLX-112 in conscious animals are shown in Figure 2A. Regarding activation maps, clusters were detected in the parietal, insular, and ectorhinal cortices for all doses. A strong activation was also observed in the pontine nuclei at 0.32 mg/kg and 0.63 mg/kg and in the cerebellum at 0.63 mg/kg. Clusters with a significant decrease of [^{18}F]FDG uptake ratio compared to saline injection were found in the brainstem, the piriform cortex, and the striatum for all doses and in the ventral hippocampus and the posterior cingulate cortex at the highest dose. Similar results were observed in the volume of interest (VOI) analysis (Figure 2B). A dose-dependent increase of [^{18}F]FDG uptake ratio compared to the saline injection was detected in the parietal cortex (from +6.65% at 0.16 mg/kg to +11.77% at 0.63 mg/kg) and in the cerebellum (from +3.07% at 0.16 mg/kg to +16.27% at 0.63 mg/kg). Other significant activations were found in the insular cortex at 0.16 mg/kg (+7.3%) and in the pontine nuclei at 0.63 mg/kg (+17.75%) of NLX-112. A dose-dependent decrease of relative [^{18}F]FDG uptake was observed in the striatum (from −3.87% at 0.16 mg/kg to −8.43% at 0.63 mg/kg) and in the piriform cortex (from −25.38% at 0.16 mg/kg to −37.97% at 0.63 mg/kg). Other significant inhibitions were also found in the brainstem at 0.63 mg/kg (−7.29%) and in the hippocampus at 0.63 mg/kg (−4.43%).

The representative images of the voxel-based analysis of the effects of NLX-101 in conscious animals are shown in Figure 3A. Significant activations were detected in the frontal cortex, the colliculi, the insular cortex, and the right dorsal

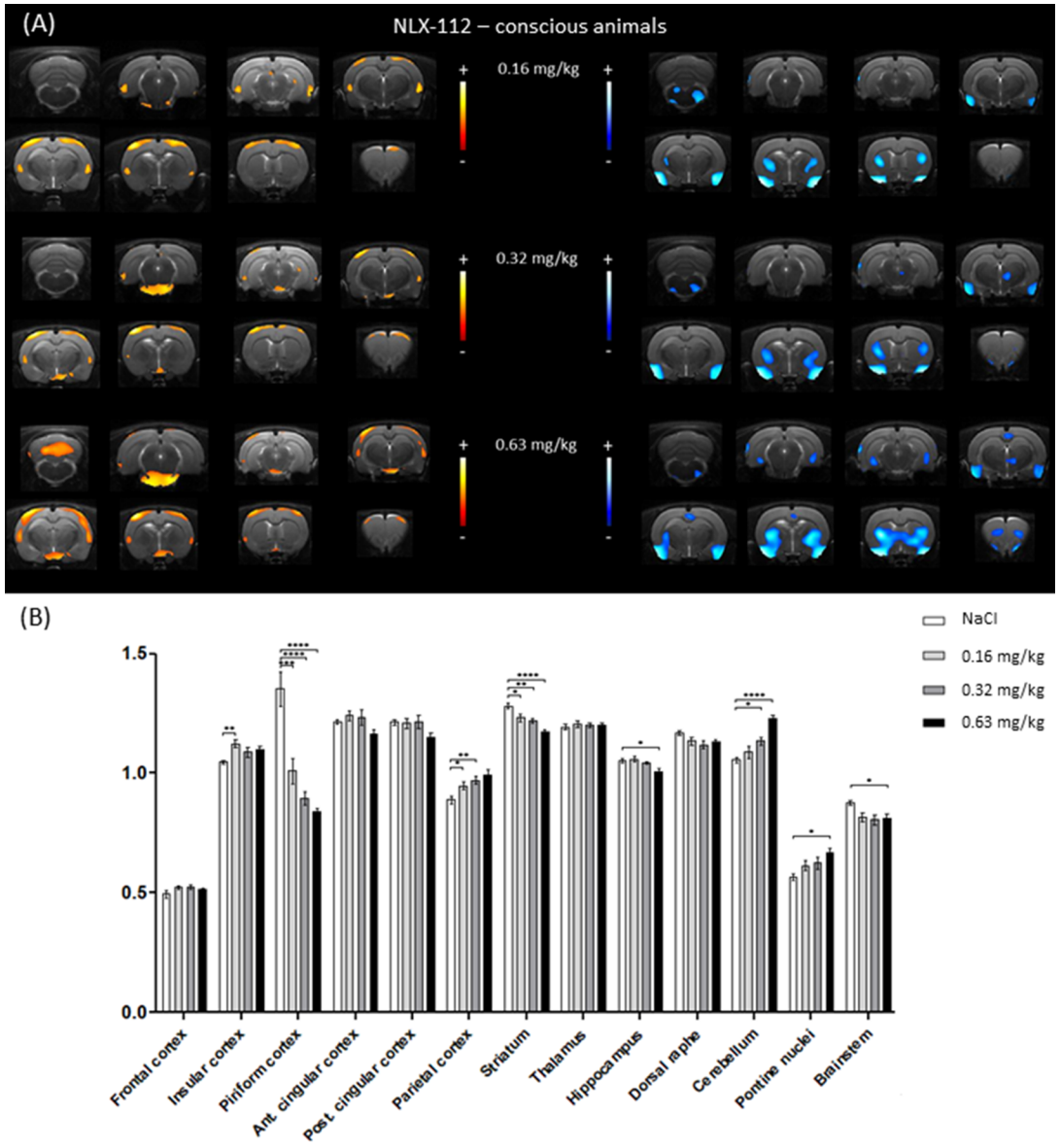

Figure 2. Effects of administration of NLX-112 at 0.16, 0.32, and 0.63 mg/kg on glucose metabolism in conscious rats (n = 9). (A) Voxel-to-voxel statistical comparisons of [^{18}F]FDG uptake ratio between NLX-112 injections and NaCl injection. On the left, significant increases of glucose metabolism; on the right, images showing a decrease of glucose metabolism in rats injected with NLX-112 at different doses compared to NaCl. (B) [18F]FDG uptake ratios in several VOIs after NLX-112 or saline injection (expressed as uptake ratio, mean ± SD; *p < 0.05, **p < 0.01, ***p < 0.001, ****p < 0.0001).

hippocampus for all doses. Other increases were found in the hypothalamus and pontine nuclei at 0.32 mg/kg and 0.63 mg/kg and in the thalamus and the cerebellum at 0.63 mg/kg only. Concerning inhibition maps, significant clusters were found in the dorsal raphe and the brainstem at 0.32 and 0.63 mg/kg. [^{18}F]FDG uptake ratio was also decreased in the piriform cortex and the striatum for all doses. The VOI analysis yielded similar results (Figure 3B). A significant increase of [^{18}F]FDG uptake ratio was detected in the frontal cortex at 0.16 mg/kg (+14.12%) and 0.32 mg/kg (+13.58%) of NLX-101, while at 0.63 mg/kg, the increase was not statistically significant (+10.27%). Other increases were detected in the insular cortex at 0.32 (+9.83%) and 0.63 mg/kg (+9.57%) and in the cerebellum (+8.21%) at 0.63 mg/kg. A dose-dependent decrease of relative glucose uptake was observed in the piriform cortex (from −23.67% at 0.16 mg/kg to −30.86% at 0.63 mg/kg). Other significant decreases were found in the striatum (−3.12% at 0.32 mg/kg and −5.12% at 0.63 mg/kg), in the dorsal raphe at 0.63 mg/kg (−6.40%), and in the brainstem at all doses (−8.95% at 0.16 mg/kg, −9.18% at 0.32 mg/kg, and −8.89 at 0.63 mg/kg).

Taken together, these results show that NLX-112 and NLX-101 have distinct effects on cerebral glucose metabolism *in vivo* (see Figure 4 for a summary of the main differences). In certain regions, both NLX-112 and NLX-101 induced significant changes of [^{18}F]FDG uptake ratio, but the effect of NLX-112 was greater at equal doses. For instance, both molecules strongly decreased the relative [^{18}F]FDG uptake ratio in the piriform cortex, but the inhibition induced by NLX-112 was from 1.1 to 1.2 times greater than that induced by NLX-101. In the striatum, the maximal effect of NLX-101 was about half the effect observed with NLX-112. In the

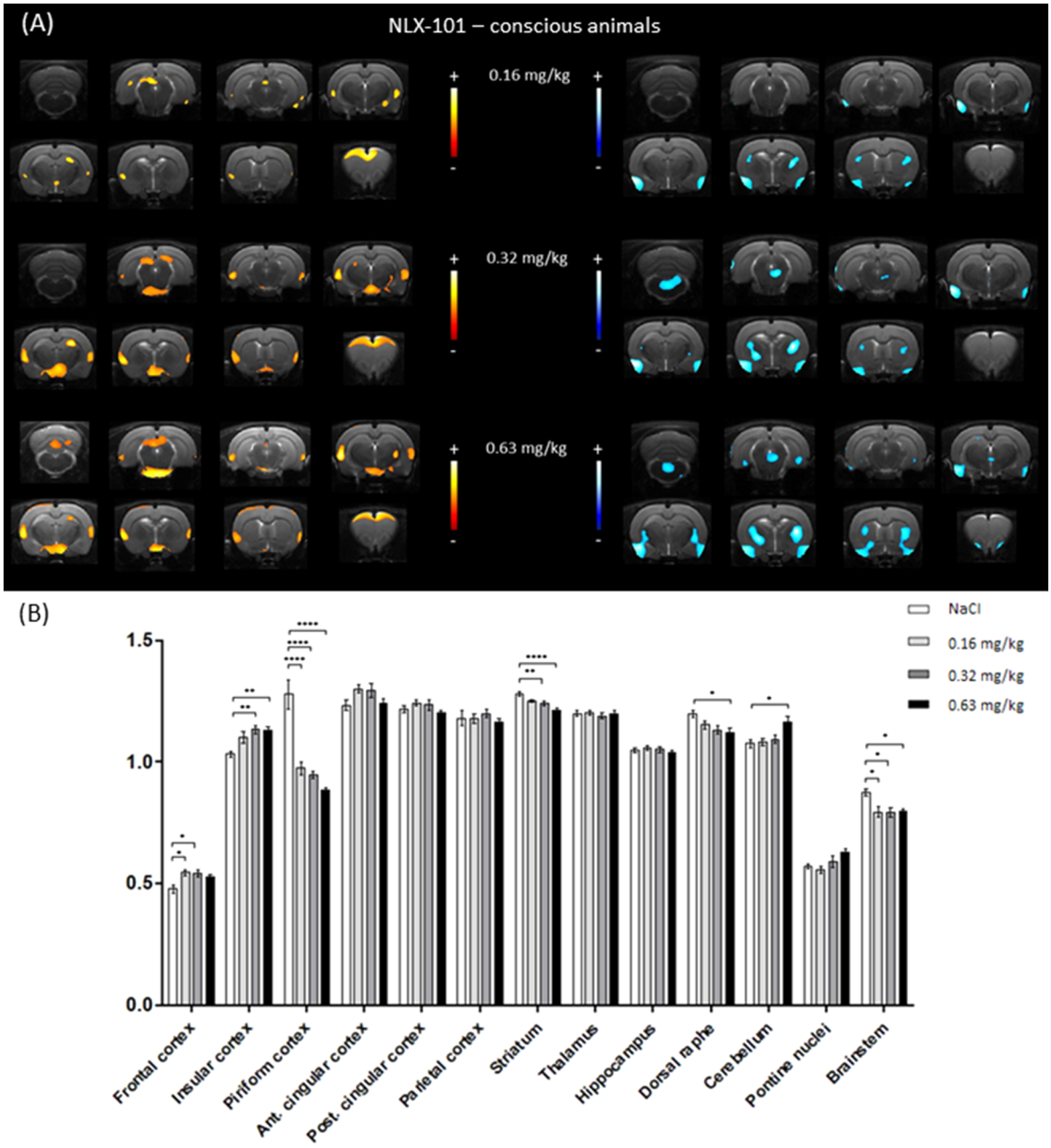

Figure 3. Effects of administration of NLX-101 at 0.16, 0.32, and 0.63 mg/kg on glucose metabolism in conscious rats (n = 7). (A) Voxel-to-voxel statistical comparisons of [^{18}F]FDG uptake ratio between NLX-101 injections and NaCl injection. On the left: significant increases of glucose metabolism; on the right, images showing a decrease of glucose metabolism in rats injected with NLX-101 at different doses compared to NaCl. (B) [^{18}F]FDG uptake ratios in several VOIs after NLX-101 or saline injection (expressed as uptake ratio, mean ± SD; *p < 0.05, **p < 0.01, ***p < 0.001, ****p < 0.0001).

cerebellum, the increase of glucose metabolism induced by 0.63 mg/kg of NLX-112 was also 2 times more pronounced than that with NLX-101. NLX-112 also induced a higher activation in the pontine nuclei than NLX-101, whereas only NLX-101 produced a strong activation in the hypothalamus at 0.32 mg/kg and 0.63 mg/kg. In other regions, the differences between agonists were even more obvious. NLX-101 induced a clear activation in the frontal cortex at all doses, whereas NLX-112 was devoid of effect at any dose in this region. Similarly, in the insular cortex NLX-101 dose-dependently increased [^{18}F]FDG uptake ratio, whereas only the lowest dose of NLX-112 had a significant effect. In addition, in the voxel-based analysis only NLX-101 produced a significant activation in the colliculi at all doses, whereas NLX-112 did not produced relative changes in this region at any dose. In contrast, NLX-112 administration was followed by a dose-dependent increase of relative glucose uptake in the parietal cortex (motor and somatosensory areas), whereas NLX-101 did not modify [^{18}F]FDG uptake ratio in this region at any dose (only very few voxels found activated at 0.63 mg/kg and no changes in the VOI analysis). Moreover, NLX-112 (0.63 mg/kg) elicited a decrease of glucose metabolism in the posterior cingulate cortex not observed with NLX-101, and NLX-112 tended to decrease the relative glucose uptake in the ventral hippocampus, whereas NLX-101 tended to increase it in the dorsal hippocampus. All these observations suggest that despite acting

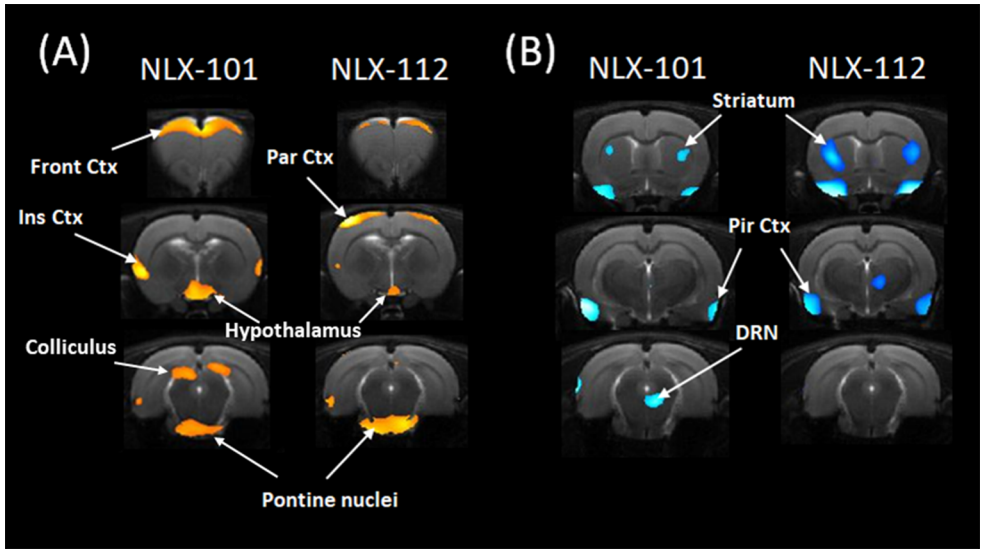

Figure 4. Differential effects of NLX-101 and NLX-112 on cerebral glucose metabolism in conscious rats. Results are shown for the dose of 0.32 mg/kg but were similar at other doses. (A) Significant increases of glucose metabolism induced by NLX-101 (on the left) or NLX-112 (on the right). Only NLX-112 produced an activation in the parietal cortex, whereas only NLX-101 produced an activation in the colliculi and in the frontal cortex; both agonists increased the glucose uptake in the insular cortex, in the pontine nuclei, and in the hypothalamus. (B) Significant decreases of glucose metabolism induced by NLX-101 (on the left) or NLX-112 (on the right). NLX-112 induced greater decreases of glucose metabolism in the striatum and the piriform cortex, whereas the inhibition in the dorsal raphe was detected only with NLX-101.

on the same type of receptors, NLX-112 and NLX-101 have different pharmacological properties *in vivo* and may act preferentially on distinct subpopulations of receptors. Given the known distribution of 5-HT_{1A} R and the inhibitory nature of the G-proteins interacting with these receptors, the inhibition of cerebral glucose metabolism observed in the hippocampus and the cingulate cortex (for NLX-112 at 0.63 mg/kg) or the dorsal raphe nucleus (for NLX-101) is likely to be due to direct stimulation of 5-HT_{1A} receptors in these regions. It is surprising that only NLX-101 produced a local decrease in the dorsal raphe since other preclinical data suggest that NLX-112 activates more potently presynaptic 5-HT_{1A} receptors than NLX-101,[10] including another imaging study that we recently performed in cat brain using simultaneous PET and pharmacological MRI.[19] This absence of clear effect may be explained by a partial volume effect: the larger increase of relative [^{18}F]FDG uptake that NLX-112 produced in the pontine nuclei (compared to NLX-101) may partially hide its inhibitory effect in the dorsal raphe due to the proximity between these regions and the low resolution of the microPET. Concerning NLX-101, although previous data show that it has a preference for cortical postsynaptic receptors, some data also suggest that it activates 5-HT_{1A} autoreceptors at doses above 0.16 mg/kg;[34] this underlines the importance of the choice of dose to target selectively certain populations of receptors. Interestingly, only NLX-101 produced a local activation in the frontal cortex. This result is consistent with previous works on the molecule suggesting it is able to preferentially activate postsynaptic receptors in the frontal cortex, a biased agonist effect, which is associated with its procognitive properties that are not shared with several other 5-HT_{1A} receptor agonists.[17,32,33] This is also consistent with our results in cat showing that only NLX-101 induced an increase of BOLD signal in response to 5-HT_{1A} receptor occupancy in the anterior cingulate cortex, whereas NLX-112 produced an opposite effect.[19]

Although the insular cortex, the brainstem, and especially the striatum are not usually described as rich in 5-HT_{1A} receptors, the relative changes of glucose uptake in these regions could also be due to a direct stimulation of 5-HT_{1A} receptors. Indeed, previous experiments using radiolabeled [^{18}F]NLX-112 and [^{18}F]NLX-101 showed a significant uptake of both compounds in these regions in rat brain, suggesting that they contain a population of highly functional 5-HT_{1A} receptors.[39,40] Interestingly, the pronounced inhibition observed with NLX-112 in the striatum may be related to its powerful antidyskinetic effect,[35] as it has been shown that a striatal microinjection of 5-HT_{1A} agonists is able to block the expression of L-DOPA-induced dyskinesia in hemiparkinsonian rats.[41,42] Similarly, the brainstem has been suggested as a key region for the prorespiratory effects of both molecules.[43,44]

It has to be kept in mind that regional changes in cerebral glucose metabolism could also be due to indirect modulation of other neuronal populations interacting with those expressing 5-HT_{1A} receptors. In particular, the stimulation of 5-HT_{1A} autoreceptors in the raphe could induce widespread metabolic changes by reducing serotonin release in serotonergic projection areas.[45] The influence of endogenous serotonin on cerebral glucose metabolism has been previously demonstrated by experiments in human brain using the serotonin releaser fenfluramine[26,27] or the selective serotonin reuptake inhibitor citalopram,[28] and in conscious rat via a direct electrical stimulation of raphe nuclei.[46] In particular, serotonergic neurons are involved in olfactory processing, and the stimulation of raphe nuclei triggers the excitation of olfactory cells.[47] Olfactory cells are known to interact with the piriform cortex in the behavioral response to olfactory stimuli;[48] therefore, the strong local decrease that we found in the piriform cortex might be indirectly due to the inhibition of serotonergic neurons following the stimulation of 5-HT_{1A} autoreceptors. According to this hypothesis, the effect of NLX-112 on autoreceptors would be higher than that of NLX-101, despite not being directly detected in the raphe.

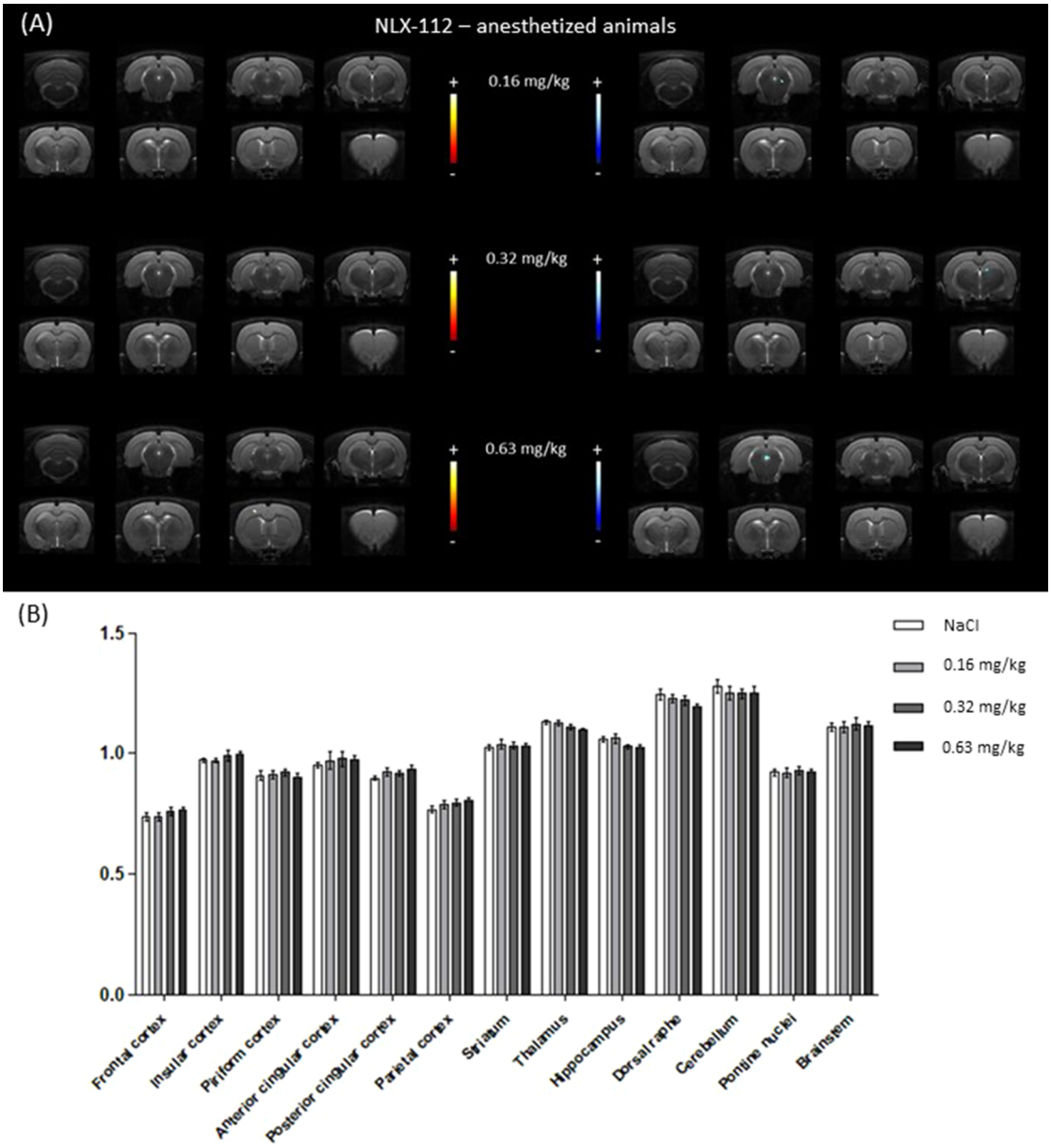

Figure 5. Effects of administration of NLX-112 at 0.16, 0.32, and 0.63 mg/kg on glucose metabolism in anesthetized rats (n = 8). (A) Voxel-to-voxel statistical comparisons of [^{18}F]FDG uptake ratio between NLX-112 injections and NaCl injection. On the left, significant increases of glucose metabolism; on the right, images showing a decrease of glucose metabolism in rats injected with NLX-112 at different doses compared to NaCl. (B) [^{18}F]FDG uptake ratios in several VOIs after NLX-112 or saline injection (expressed as uptake ratio, mean ± SD). There was no statistical difference of radiotracer uptake in any VOI between NLX-112 or NaCl.

The behavioral effects of the drugs are also likely to produce strong effects on glucose metabolism in areas involved in somatosensory and motor processes, without a specific link with 5-HT$_{1A}$ receptors.[37] This could explain why both agonists induced an increase of glucose metabolism in the cerebellum, given that they tended to increase the motor behavior of rats. NLX-112, in particular, had prominent behavioral effects and was associated with some signs of serotonergic syndrome at 0.63 mg/kg, which may explain why it increased the glucose uptake ratio in the motor and somatosensory cortices.

PET Scans Performed in Anesthetized Rats. For NLX-112, representative images of the voxel-based analysis in isoflurane-anesthetized animals are shown in Figure 5A: almost no statistically significant differences were detected when comparing the different doses of NLX-112 and NaCl 0.9% in anesthetized animals. Regarding activation maps, only few nonsymmetric clusters with size inferior to 0.34 mm^3 were detected in the frontal and insular cortices in animals injected with 0.63 mg/kg compared to NaCl (data not shown). Concerning inhibition maps, only few unilateral clusters with size inferior to 1.8 mm^3 were detected in the hippocampus and the thalamus (data not shown) for all three doses. Figure 5B represents data obtained in the VOI analysis. No significant differences of [^{18}F]FDG uptake ratio were detected between the saline injection and the different doses of NLX-112.

For NLX-101, representative images of the voxel-based analysis in isoflurane-anesthetized animals are shown in Figure 6A. Regarding activation maps, only one cluster of 1.53 mm^3 was found in the right ectorhinal cortex at dose of 0.63 mg/kg. Concerning inhibition maps, two clusters were detected in the

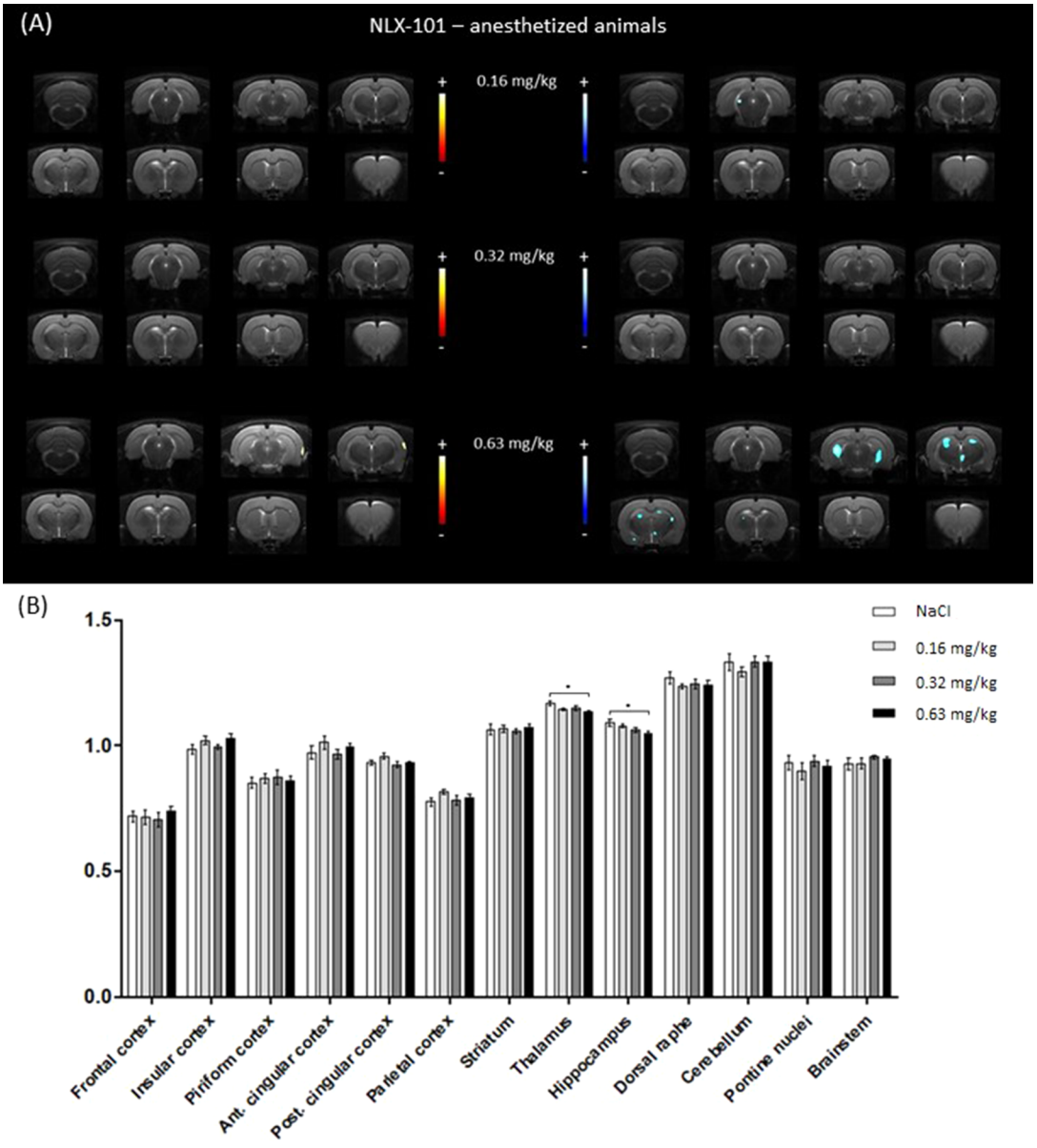

Figure 6. Effects of administration of NLX-101 at 0.16, 0.32, and 0.63 mg/kg on glucose metabolism in anesthetized rats (n = 7). (A) Voxel-to-voxel statistical comparisons of [^{18}F]FDG uptake ratio between NLX-101 injections and NaCl injection. On the left, significant increases of glucose metabolism; on the right, images showing a decrease of glucose metabolism in rats injected with NLX-101 at different doses compared to NaCl. (B) [^{18}F]FDG uptake ratios in several VOIs after NLX-101 or saline injection (expressed as uptake ratio, mean ± SD; *p < 0.05).

colliculus and in the thalamus at 0.16 mg/kg of NLX-101 (data not shown). Other decreases of [^{18}F]FDG uptake ratio were detected in the hippocampus and in the thalamus at 0.63 mg/kg of NLX-101 (Figure 6A). Figure 6B represents data obtained in the VOI analysis. Significant decreases in [^{18}F]FDG uptake ratio were observed in the thalamus (−1.32%) and in the hippocampus (−1.67%) when rats were injected with 0.63 mg/kg of NLX-101.

Therefore, neither NLX-112 nor NLX-101 elicited [^{18}F]FDG uptake ratio changes during anesthesia in a manner that was comparable to the results obtained in conscious rats. Such striking differences may be explained by several factors. First, global cerebral glucose metabolism is reduced under isoflurane, reflecting a global decrease of neuronal activity that would reduce the influence of 5-HT$_{1A}$ agonists (a decrease of 54% of [^{18}F]FDG uptake was observed in anesthetized animals compared to conscious animals in control condition in the present study). Moreover, in addition to this global decrease, isoflurane anesthesia induced profound changes of [^{18}F]FDG uptake pattern, as compared to the awake condition (Figure 7). Representative images of the voxel-based analysis (Figure 7A) showed that isoflurane anesthesia locally increased glucose metabolism in the frontal cortex, the dorsal raphe, the cerebellum, the pontine nuclei, and the brainstem, as compared to the whole brain. Conversely, a decreased metabolism was observed in the insular, piriform, cingulate, and parietal cortices, in the striatum, and in the thalamus compared to the rest of the brain. The VOI analysis showed that these differences in local uptake were important (Figure 7B), with an increase of 6.31% in the dorsal raphe, 17.01% in the brainstem, 22.40% in the cerebellum, 49.55% in the frontal cortex, and up to 62.94% in the pontine nuclei compared to the conscious state, and a decrease of 4.02% in the thalamus, 5.96% in the insular cortex, 23.06% and 24.59% in the

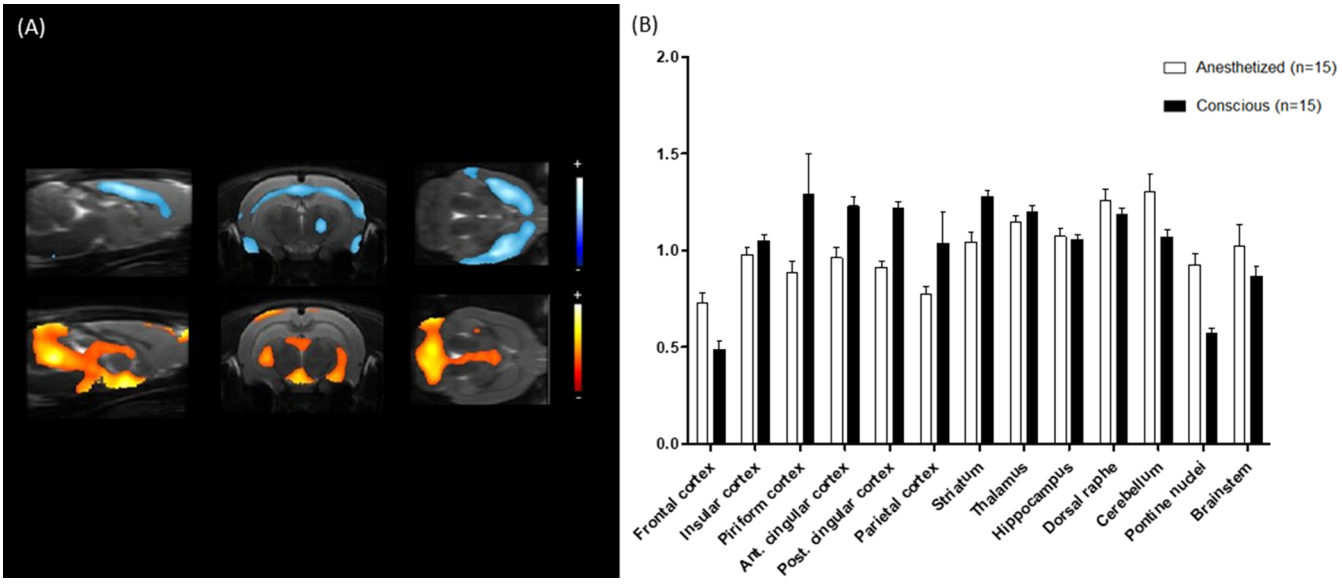

Figure 7. Effects of isoflurane anesthesia on glucose metabolism. (A) Representative local differences of glucose metabolism between the animals kept under isoflurane anesthesia or awake during the [^{18}F]FDG uptake period. The blue color bar indicates a local increase of glucose uptake in conscious rats versus anesthetized rats, and the red to yellow bar indicates a local increase of glucose uptake in anesthetized rats versus conscious animals. (B) Brain regions with significant difference of [^{18}F]FDG uptake between the isoflurane anesthesia and the awake conditions (except for hippocampus, difference was not significant).

cingulate and parietal cortices, and 32.96% in the piriform cortex. These results are consistent with a previous study that was also performed in male Sprague–Dawley rats[49] and suggest that regions are differently impacted by isoflurane anesthesia with some regions (such as the cortex) that are particularly affected, an important consideration when mapping the functional effects of CNS ligands. Another explanation for the lack of effect of NLX-101 and NLX-112 in anesthetized rats is that the behavioral effects that can be observed in the conscious rats are blocked during anesthesia. Consequently, no more changes of [^{18}F]FDG uptake ratio are observed in regions involved in motor or sensory functions such as the cerebellum and the motor or somatosensory cortices. Furthermore, isoflurane is known to impact serotonergic neurotransmission by decreasing the activity of serotonergic neurons[20] and the liberation of endogenous serotonin,[50] thus reducing the impact of 5-HT$_{1A}$ autoreceptor stimulation. Finally, it might be possible that isoflurane directly alters the functional state of 5-HT$_{1A}$ receptors: although the impact of isoflurane on the coupling between 5-HT$_{1A}$ receptors and G-proteins is poorly characterized, it was previously reported to inhibit the coupling between D2, D3, 5-HT$_{2A}$, β-2, α-1, α-2, opiate, muscarinic receptors, and their G-proteins.[51] This question is important for the concept of biased agonism, as different signaling pathways may be differentially altered by anesthetics. In this regard, in a PET study in marmoset, the binding kinetics of the 5-HT$_{1A}$ agonist [^{18}F]F13714 (a chemical congener of NLX-112 and NLX101) showed region-specific changes in isoflurane-anesthetized animals compared to conscious animals,[22] although this could be interpreted in terms of local differences in endogenous serotonin levels. As a conclusion, this study emphasizes the strong impact of anesthesia on pharmacological imaging, which may limit the interpretation of results for many preclinical studies. [^{18}F]FDG PET imaging offers the opportunity to explore the central effects of drugs in nonanesthetized animals easily, facilitating the clinical extrapolation of findings.

METHODS

Animals. Thirty-one male Sprague–Dawley adult rats (Charles River laboratories, France) weighing 337.89 ± 41.23 g were used in this protocol. The animals were hosted in standard temperature and humidity conditions with a 12 h/12 h light/dark cycle. Food and water were provided *ad libitum*. All experiments were performed in accordance with the European guidelines for care of laboratory animals (2010/63/EU) and were approved by the University of Lyon review board.

PET/CT Imaging. Each animal underwent 4 different PET scans, with a control condition (injection of NaCl 0.9%) and NLX-112 or NLX-101 at three distinct doses: 0.16 mg/kg, 0.32 mg/kg, and 0.63 mg/kg. A minimum of 48 h between scans was observed. All rats were fasted during 4 h before experiments. For the conscious group (n = 9 for NLX-112 and n = 7 for NLX-101), intraperitoneal injection of NLX-112, NLX-101, or NaCl 0.9% was performed. Fifteen minutes later, when the central effects of the drugs were prominent, catheterization of the caudal vein was performed, and [^{18}F]FDG was injected in awake animals (no transient anesthesia to facilitate the tracer injection). After 30 min of uptake, isoflurane was used at 4% for induction followed by a continuous insufflation at 2%. As [^{18}F]FDG is transported into the brain within minutes and rapidly converted into [^{18}F]FDG-6-P, which is "trapped" in the cells for several hours,[52,53] we consider that the induction of anesthesia just before the PET scan has no consequence on the brain glucose uptake that we measured in the conscious group. The same timeline was used for the anesthetized group (n = 8 for NLX-112 and n = 7 for NLX-101), but isoflurane was used during the whole experiment. The intraperitoneal injection of NLX-112, NLX-101, or NaCl 0.9% was realized just after the induction of anesthesia.

Following the [^{18}F]FDG uptake period, the rat head was centered in the field of view (FOV) of the PET/CT scanner (Inveon, Siemens, Knoxville, TN, USA). PET scans were acquired in list mode during 30 min, with a nominal in-plane resolution of ∼1.4 mm full width at half-maximum in the center of the FOV. A CT scan was performed in the same position immediately after PET emission scan to correct for tissue attenuation. Breathing and heart rates were continuously monitored during the imaging session.

Static images of the 30 min acquisitions were reconstructed with attenuation and scatter correction by 3D ordinary Poisson ordered

subsets expectation-maximization (OP-OSEM3D) with 4 iterations and a zoom factor of 2. The reconstructed volume was constituted of 159 slices of 128 × 128 voxels, in a bounding box of 49.7 × 49.7 × 126 mm^3 and with voxel size 0.388 × 0.388 × 0.796 mm^3 OSEM 3D. The images were analyzed with the INVEON research Workplace (IRW, Siemens).

The radiopharmaceutical [^{18}F]FDG (GlucoTEP and Gluscan) was obtained from Cyclopharma (Janneyrias, France) and Advanced Accelerator Applications (Saint Genis Pouilly, France), respectively. The injected doses of [^{18}F]FDG were 9.9 ± 1.4 MBq.

Voxel-Based Analysis (VBA). Data processing was carried out using the statistical parametric mapping software (SPM12, Wellcome Trust Center for Neuroimaging, London; UK). Individual PET images were realigned and spatially normalized on a custom PET [^{18}F]FDG template, which was co-registered on an anatomical MRI template.[54] Each PET volume was smoothed using an isotropic Gaussian filter [1 × 1 × 1 mm^3]. Global activities were normalized to the mean uptake of the whole brain to obtain a ratio. For each group (NLX-112 and NLX-101 in anesthetized and awake groups), a statistical analysis was performed to compare mean uptakes between saline and 5-HT_{1A} molecule conditions in each individual. This ANOVA resulted in activation (contrast, [5-HT_{1A} agonist − control]) and inhibition (contrast, [control − 5-HT_{1A} agonist)] maps for each dose of molecule and each condition (awake/anesthesia). A significant threshold was set up at $p < 0.001$ uncorrected. A second analysis using an unpaired t test was performed to compare NaCl conditions between awake ($n = 15$) and anesthetized rats ($n = 15$) in order to evaluate the direct influence of isoflurane on [^{18}F]FDG uptake ratio ($p < 0.001$ uncorrected).

Volume of Interest (VOI) Analysis. VOIs were manually drawn from clusters identified on activation and inhibition maps or already defined in the Lancelot rat brain atlas on the corresponding MRI template.[54] Mean uptake ratios were extracted in the different VOIs, and a one-way ANOVA with Bonferroni post hoc tests were performed using GraphPad Prism 5.0 software to compare the [^{18}F]FDG uptake ratios between the different doses of agonists and saline. Mann−Whitney tests were performed to compare the conscious state with the anesthetized state in the control condition. Values were considered to be significantly different for p-values lower than 0.05.

AUTHOR INFORMATION

Corresponding Author

*E-mail: luc.zimmer@univ-lyon1.fr. Phone: +33 4 72 68 86 09. Fax: +33 4 72 68 86 10.

ORCID

Elise Levigoureux: 0000-0003-1231-1036

Adrian Newman-Tancredi: 0000-0002-2923-5714

Luc Zimmer: 0000-0002-2805-7098

Author Contributions

#E.L. and B.V. contributed equally to this work. E.L. and B.V. carried out the experiments with PET imaging, performed data analysis, participated in the study design, and cowrote the manuscript. S.F. and C.B. carried out the experiments with PET imaging and participated in data analysis. S.E. performed radiopharmaceutical preparations. A.N.-T. provided NLX-112 and NLX-101 and reviewed the manuscript. L.Z. initiated the study, participated in its design, and reviewed the manuscript. All authors read and approved the final manuscript.

Funding

This work was performed within the framework of the LABEX PRIMES (ANR-11-LABX-0063) of Université de Lyon, within the program "Investissements d'Avenir" (ANR-11-IDEX-0007) operated by the French National Research Agency (ANR).

Notes

The authors declare the following competing financial interest(s): Dr. Newman-Tancredi is an employee and stockholder of Neurolixis. The other authors report no conflict of interest and have nothing to disclose.

ACKNOWLEDGMENTS

We thank Jérôme Redouté for his help in the data analysis and Véronique Gualda for the zootechnical assistance.

REFERENCES

(1) Lacivita, E., Di Pilato, P., De Giorgio, P., Colabufo, N. A., Berardi, F., Perrone, R., and Leopoldo, M. (2012) The therapeutic potential of 5-HT1A receptors: a patent review. *Expert Opin. Ther. Pat. 22*, 887−902.

(2) Kaufman, J., DeLorenzo, C., Choudhury, S., and Parsey, R. V. (2016) The 5-HT1A receptor in Major Depressive Disorder. *Eur. Neuropsychopharmacol. 26*, 397−410.

(3) McCreary, A. C., and Newman-Tancredi, A. (2015) Serotonin 5-HT1A Receptors and Antipsychotics - An Update in Light of New Concepts and Drugs. *Curr. Pharm. Des. 21*, 3725−3731.

(4) Feighner, J. P., and Boyer, W. F. (1989) Serotonin-1A anxiolytics: an overview. *Psychopathology 22* (Suppl 1), 21−26.

(5) Politis, M., Wu, K., Loane, C., Brooks, D. J., Kiferle, L., Turkheimer, F. E., Bain, P., Molloy, S., and Piccini, P. (2014) Serotonergic mechanisms responsible for levodopa-induced dyskinesias in Parkinson's disease patients. *J. Clin. Invest. 124*, 1340−1349.

(6) Verdurand, M., and Zimmer, L. (2017) Hippocampal 5-HT1A receptor expression changes in prodromal stages of Alzheimer's disease: Beneficial or deleterious? *Neuropharmacology 123*, 446−454.

(7) Andrade, R., Huereca, D., Lyons, J. G., Andrade, E. M., and McGregor, K. M. (2015) 5-HT1A Receptor-Mediated Autoinhibition and the Control of Serotonergic Cell Firing. *ACS Chem. Neurosci. 6*, 1110−1115.

(8) Lanfumey, L., and Hamon, M. (2000) Central 5-HT(1A) receptors: regional distribution and functional characteristics. *Nucl. Med. Biol. 27*, 429−435.

(9) Polter, A. M., and Li, X. (2010) 5-HT1A receptor-regulated signal transduction pathways in brain. *Cell. Signalling 22*, 1406−1412.

(10) Newman-Tancredi, A. (2011) Biased agonism at serotonin 5-HT1A receptors: preferential postsynaptic activity for improved therapy of CNS disorders. *Neuropsychiatry 1*, 149−164.

(11) la Cour, C. M., El Mestikawy, S., Hanoun, N., Hamon, M., and Lanfumey, L. (2006) Regional differences in the coupling of 5-hydroxytryptamine-1A receptors to G proteins in the rat brain. *Mol. Pharmacol. 70*, 1013−1021.

(12) Kenakin, T., and Christopoulos, A. (2012) Signalling bias in new drug discovery: detection, quantification and therapeutic impact. *Nat. Rev. Drug Discovery 12*, 205−216.

(13) Newman-Tancredi, A., Martel, J. C., Assie, M. B., Buritova, J., Lauressergues, E., Cosi, C., Heusler, P., Bruins Slot, L., Colpaert, F. C., Vacher, B., and Cussac, D. (2009) Signal transduction and functional selectivity of F15599, a preferential post-synaptic 5-HT1A receptor agonist. *Br. J. Pharmacol. 156*, 338−353.

(14) Newman-Tancredi, A., Martel, J. C., Cosi, C., Heusler, P., Lestienne, F., Varney, M. A., and Cussac, D. (2017) Distinctive in vitro signal transduction profile of NLX-112, a potent and efficacious serotonin 5-HT1A receptor agonist. *J. Pharm. Pharmacol. 69*, 1178−1190.

(15) Buritova, J., Berrichon, G., Cathala, C., Colpaert, F., and Cussac, D. (2009) Region-specific changes in 5-HT1A agonist-induced Extracellular signal-Regulated Kinases 1/2 phosphorylation in rat brain: a quantitative ELISA study. *Neuropharmacology 56*, 350−361.

(16) Llado-Pelfort, L., Assie, M. B., Newman-Tancredi, A., Artigas, F., and Celada, P. (2012) In vivo electrophysiological and neurochemical effects of the selective 5-HT1A receptor agonist,

F13640, at pre- and postsynaptic 5-HT1A receptors in the rat. *Psychopharmacology (Berl) 221*, 261−272.
(17) Llado-Pelfort, L., Assie, M. B., Newman-Tancredi, A., Artigas, F., and Celada, P. (2010) Preferential in vivo action of F15599, a novel 5-HT(1A) receptor agonist, at postsynaptic 5-HT(1A) receptors. *Br. J. Pharmacol. 160*, 1929−1940.
(18) Vidal, B., Bolbos, R., Redouté, J., Langlois, J. B., Fieux, S., Bouillot, C., Costes, N., Newman-Tancredi, A., and Zimmer, L. (2017) 5-HT1A biased agonists induce different hemodynamic responses: a pharmacological MRI study. *Eur. Neuropsychopharmacol. 27*, S642−S643.
(19) Vidal, B., Fieux, S., Redoute, J., Villien, M., Bonnefoi, F., Le Bars, D., Newman-Tancredi, A., Costes, N., and Zimmer, L. (2018) In vivo biased agonism at 5-HT1A receptors: characterisation by simultaneous PET/MR imaging. *Neuropsychopharmacology 43*, 2310−2319.
(20) Maurel, J. L., Autin, J. M., Funes, P., Newman-Tancredi, A., Colpaert, F., and Vacher, B. (2007) High-efficacy 5-HT1A agonists for antidepressant treatment: a renewed opportunity. *J. Med. Chem. 50*, 5024−5033.
(21) Tokugawa, J., Ravasi, L., Nakayama, T., Lang, L., Schmidt, K. C., Seidel, J., Green, M. V., Sokoloff, L., and Eckelman, W. C. (2007) Distribution of the 5-HT(1A) receptor antagonist [(18)F]FPWAY in blood and brain of the rat with and without isoflurane anesthesia. *Eur. J. Nucl. Med. Mol. Imaging 34*, 259−266.
(22) Yokoyama, C., Mawatari, A., Kawasaki, A., Takeda, C., Onoe, K., Doi, H., Newman-Tancredi, A., Zimmer, L., and Onoe, H. (2016) Marmoset Serotonin 5-HT1A Receptor Mapping with a Biased Agonist PET Probe 18F-F13714: Comparison with an Antagonist Tracer 18F-MPPF in Awake and Anesthetized States. *Int. J. Neuropsychopharmacol. 19*, pyw079.
(23) Massey, C. A., Iceman, K. E., Johansen, S. L., Wu, Y., Harris, M. B., and Richerson, G. B. (2015) Isoflurane abolishes spontaneous firing of serotonin neurons and masks their pH/CO(2) chemosensitivity. *J. Neurophysiol. 113*, 2879−2888.
(24) Arthurs, O. J., and Boniface, S. (2002) How well do we understand the neural origins of the fMRI BOLD signal? *Trends Neurosci. 25*, 27−31.
(25) Wehrl, H. F., Hossain, M., Lankes, K., Liu, C. C., Bezrukov, I., Martirosian, P., Schick, F., Reischl, G., and Pichler, B. J. (2013) Simultaneous PET-MRI reveals brain function in activated and resting state on metabolic, hemodynamic and multiple temporal scales. *Nat. Med. 19*, 1184−1189.
(26) Oquendo, M. A., Krunic, A., Parsey, R. V., Milak, M., Malone, K. M., Anderson, A., van Heertum, R. L., and John Mann, J. (2005) Positron emission tomography of regional brain metabolic responses to a serotonergic challenge in major depressive disorder with and without borderline personality disorder. *Neuropsychopharmacology 30*, 1163−1172.
(27) Soloff, P. H., Meltzer, C. C., Becker, C., Greer, P. J., and Constantine, D. (2005) Gender differences in a fenfluramine-activated FDG PET study of borderline personality disorder. *Psychiatry Res., Neuroimaging 138*, 183−195.
(28) Munro, C. A., Workman, C. I., Kramer, E., Hermann, C., Ma, Y., Dhawan, V., Chaly, T., Eidelberg, D., and Smith, G. S. (2012) Serotonin modulation of cerebral glucose metabolism: sex and age effects. *Synapse 66*, 955−964.
(29) Jenkins, B. G. (2012) Pharmacologic magnetic resonance imaging (phMRI): imaging drug action in the brain. *NeuroImage 62*, 1072−1085.
(30) Bardin, L., Tarayre, J. P., Malfetes, N., Koek, W., and Colpaert, F. C. (2003) Profound, non-opioid analgesia produced by the high-efficacy 5-HT(1A) agonist F 13640 in the formalin model of tonic nociceptive pain. *Pharmacology 67*, 182−194.
(31) Bardin, L., Assie, M. B., Pelissou, M., Royer-Urios, I., Newman-Tancredi, A., Ribet, J. P., Sautel, F., Koek, W., and Colpaert, F. C. (2004) Dual, hyperalgesic, and analgesic effects of the high-efficacy 5-hydroxytryptamine 1A (5-HT1A) agonist F 13640 [(3-chloro-4-fluoro-phenyl)-[4-fluoro-4-{[(5-methyl-pyridin-2-ylmethyl)-amino]-me thyl}piperidin-1-yl]methanone, fumaric acid salt]: relationship with 5-HT1A receptor occupancy and kinetic parameters. *J. Pharmacol. Exp. Ther. 312*, 1034−1042.
(32) Depoortere, R., Auclair, A. L., Bardin, L., Colpaert, F. C., Vacher, B., and Newman-Tancredi, A. (2010) F15599, a preferential post-synaptic 5-HT1A receptor agonist: activity in models of cognition in comparison with reference 5-HT1A receptor agonists. *Eur. Neuropsychopharmacol. 20*, 641−654.
(33) Assie, M. B., Bardin, L., Auclair, A. L., Carilla-Durand, E., Depoortere, R., Koek, W., Kleven, M. S., Colpaert, F., Vacher, B., and Newman-Tancredi, A. (2010) F15599, a highly selective post-synaptic 5-HT(1A) receptor agonist: in-vivo profile in behavioural models of antidepressant and serotonergic activity. *Int. J. Neuropsychopharmacol. 13*, 1285−1298.
(34) Iderberg, H., McCreary, A. C., Varney, M. A., Cenci, M. A., and Newman-Tancredi, A. (2015) Activity of serotonin 5-HT(1A) receptor 'biased agonists' in rat models of Parkinson's disease and L-DOPA-induced dyskinesia. *Neuropharmacology 93*, 52−67.
(35) Iderberg, H., McCreary, A. C., Varney, M. A., Kleven, M. S., Koek, W., Bardin, L., Depoortere, R., Cenci, M. A., and Newman-Tancredi, A. (2015) NLX-112, a novel 5-HT1A receptor agonist for the treatment of L-DOPA-induced dyskinesia: Behavioral and neurochemical profile in rat. *Exp. Neurol. 271*, 335−350.
(36) Sugimoto, Y., Kimura, I., Watanabe, Y., and Yamada, J. (2001) The 5-HT1A receptor agonist 8-hydroxy-2-di-n-(propylamino)tetralin (8-OH-DPAT) induces hyperglucagonemia in rats. *Biol. Pharm. Bull. 24*, 1191−1194.
(37) Kelly, P. A., Davis, C. J., and Goodwin, G. M. (1988) Differential patterns of local cerebral glucose utilization in response to 5-hydroxytryptamine agonists. *Neuroscience 25*, 907−915.
(38) Freo, U., Pietrini, P., Pizzolato, G., Furey-Kurkjian, M., Merico, A., Ruggero, S., Dam, M., and Battistin, L. (1995) Dose-dependent effects of buspirone on behavior and cerebral glucose metabolism in rats. *Brain Res. 677*, 213−220.
(39) Lemoine, L., Verdurand, M., Vacher, B., Blanc, E., Le Bars, D., Newman-Tancredi, A., and Zimmer, L. (2010) [18F]F15599, a novel 5-HT1A receptor agonist, as a radioligand for PET neuroimaging. *Eur. J. Nucl. Med. Mol. Imaging 37*, 594−605.
(40) Vidal, B., Fieux, S., Colom, M., Billard, T., Bouillot, C., Barret, O., Constantinescu, C., Tamagnan, G., Newman-Tancredi, A., and Zimmer, L. (2018) (18)F-F13640 preclinical evaluation in rodent, cat and primate as a 5-HT1A receptor agonist for PET neuroimaging. *Brain Struct. Funct. 223*, 2973−2988.
(41) Bishop, C., Krolewski, D. M., Eskow, K. L., Barnum, C. J., Dupre, K. B., Deak, T., and Walker, P. D. (2009) Contribution of the striatum to the effects of 5-HT1A receptor stimulation in L-DOPA-treated hemiparkinsonian rats. *J. Neurosci. Res. 87*, 1645−1658.
(42) Meadows, S. M., Chambers, N. E., Conti, M. M., Bossert, S. C., Tasber, C., Sheena, E., Varney, M., Newman-Tancredi, A., and Bishop, C. (2017) Characterizing the differential roles of striatal 5-HT1A auto- and hetero-receptors in the reduction of l-DOPA-induced dyskinesia. *Exp. Neurol. 292*, 168−178.
(43) Ren, J., Ding, X., and Greer, J. J. (2015) 5-HT1A receptor agonist Befiradol reduces fentanyl-induced respiratory depression, analgesia, and sedation in rats. *Anesthesiology 122*, 424−434.
(44) Abdala, A. P., Bissonnette, J. M., and Newman-Tancredi, A. (2014) Pinpointing brainstem mechanisms responsible for autonomic dysfunction in Rett syndrome: therapeutic perspectives for 5-HT1A agonists. *Front. Physiol. 5*, 205.
(45) Altieri, S. C., Garcia-Garcia, A. L., Leonardo, E. D., and Andrews, A. M. (2013) Rethinking 5-HT1A receptors: emerging modes of inhibitory feedback of relevance to emotion-related behavior. *ACS Chem. Neurosci. 4*, 72−83.
(46) Cudennec, A., Duverger, D., Serrano, A., Scatton, B., and MacKenzie, E. T. (1988) Influence of ascending serotonergic pathways on glucose use in the conscious rat brain. II. Effects of electrical stimulation of the rostral raphe nuclei. *Brain Res. 444*, 227−246.

(47) Kapoor, V., Provost, A. C., Agarwal, P., and Murthy, V. N. (2016) Activation of raphe nuclei triggers rapid and distinct effects on parallel olfactory bulb output channels. *Nat. Neurosci. 19*, 271−282.
(48) Choi, G. B., Stettler, D. D., Kallman, B. R., Bhaskar, S. T., Fleischmann, A., and Axel, R. (2011) Driving opposing behaviors with ensembles of piriform neurons. *Cell 146*, 1004−1015.
(49) Park, T. Y., Nishida, K. S., Wilson, C. M., Jaiswal, S., Scott, J., Hoy, A. R., Selwyn, R. G., Dardzinski, B. J., and Choi, K. H. (2017) Effects of isoflurane anesthesia and intravenous morphine self-administration on regional glucose metabolism ([(18) F]FDG-PET) of male Sprague-Dawley rats. *Eur. J. Neurosci 45*, 922−931.
(50) Mukaida, K., Shichino, T., Koyanagi, S., Himukashi, S., and Fukuda, K. (2007) Activity of the serotonergic system during isoflurane anesthesia. *Anesth. Analg. 104*, 836−839.
(51) Seeman, P., and Kapur, S. (2003) Anesthetics inhibit high-affinity states of dopamine D2 and other G-linked receptors. *Synapse 50*, 35−40.
(52) Phelps, M. E., Huang, S. C., Hoffman, E. J., Selin, C., Sokoloff, L., and Kuhl, D. E. (1979) Tomographic measurement of local cerebral glucose metabolic rate in humans with (F-18)2-fluoro-2-deoxy-D-glucose: validation of method. *Ann. Neurol. 6*, 371−388.
(53) Huang, S. C., Phelps, M. E., Hoffman, E. J., Sideris, K., Selin, C. J., and Kuhl, D. E. (1980) Noninvasive determination of local cerebral metabolic rate of glucose in man. *Am. J. Physiol. 238*, No. E69.
(54) Lancelot, S., Roche, R., Slimen, A., Bouillot, C., Levigoureux, E., Langlois, J. B., Zimmer, L., and Costes, N. (2014) A multi-atlas based method for automated anatomical rat brain MRI segmentation and extraction of PET activity. *PLoS One 9*, No. e109113.